



# Structural, thermal, and linear/nonlinear optical performance of PVA/CMC polymer blend doped with ZnS/V prepared at different temperatures

A. M. El-naggar<sup>1</sup> · Zein K. Heiba<sup>2</sup> · A. M. Kamal<sup>1</sup> · Omar H. Abd-Elkader<sup>1</sup> · G. Lakshminarayana<sup>3</sup> · Mohamed Bakr Mohamed<sup>2</sup>

Received: 26 July 2022 / Accepted: 6 October 2022 / Published online: 21 October 2022  
© The Polymer Society, Taipei 2022

## Abstract

PVA/CMC blend loaded with  $Zn_{0.9}V_{0.1}S$  prepared at different temperatures ( $T = 200, 300, 400$  or  $500$  °C) were synthesized utilizing solid state reaction and casting methods. Applying Rietveld method, the cell parameter, the crystallite size, and the lattice microstrain of the nanofiller  $Zn_{0.9}V_{0.1}S$  were determined at the various preparation temperatures. The elemental analysis and the distribution of the nanofillers over the blend's matrix were investigated using X-ray diffraction, SEM and FTIR techniques. The influence of ZnS/V doping on the thermal stability of PVA/CMC was explored using thermogravimetric analysis technique. The optical features for the pure and doped PVA/CMC polymer blends with ZnS/V were explored using diffused reflectance technique. The direct and indirect  $E_g$  values for PVA/CMC are 5.79 and 5.03 eV, respectively. Upon loading,  $E_g$  decreased nonmonotonically with T, reaching lowest values (4.51, 2.43) eV for nanofiller prepared at  $T = 200$  °C. The consequences of ZnS/V doping on the fluorescence intensity and emitted colors from different blends were explored. The obtained results are significant for designing novel organic/inorganic polymer blend for emerging technologies.

**Keywords** PVA/CMC · Crystallite size of ZnS/V nano · Structure · Thermal · Optical

## Introduction

Polymer blends have attracted the consideration of many researchers towards the improvement and adaptation of innovative materials [1]. Polymer blends are employed in several technological and scientific applications as a result of their optical, thermal, and electrical features [1]. Polyvinyl alcohol (PVA) has many distinctive features such as solubility in water, good film production, physical characteristics, high

hydrophilicity, non-toxicity, bio-degradability and chemical resistance [2]. Carboxymethyl cellulose (CMC) polymer is one of common cellulose derivative that has one of the hydrophilic carboxyl groups formed from hydrophobic polysaccharides backbone with a proven water-soluble characteristic [3]. CMC is a semi-crystalline material, cheap, non-toxic, biodegradable and excellent film-forming ability [3].

Zinc sulfide (ZnS) one of semiconductor materials that has a wide optical band gap ( $> 3.5$  eV) that can be employed in numerous opto-electronics proposes [4]. The physical characteristics of ZnS can be modified upon doping with appropriate elements and/ or changing formation temperature etc. [5]. In addition, vanadium (V) ion is one of the transition metals that has numerous oxidation states from +2 to +5 [6].  $V^{5+}$  is considered the most stable ions between other vanadium ions therefore it can be employed be in catalysis, sensors, and lithium-ion battery applications [6]. Previously, we found that the optical band gap of nano  $Zn_{0.9}V_{0.1}S$  was reduced irregularly as the preparation temperature rose from 200 to 500 °C [7].

Polymer blends loaded with nanoparticles have attracted great attention in the previous years as a result of combination

✉ Zein K. Heiba  
zein\_kh@yahoo.com

✉ Mohamed Bakr Mohamed  
mbm1977@yahoo.com

<sup>1</sup> Physics & Astronomy Department, College of Science, King Saud University, P.O. Box 2455, Riyadh 11451, Saudi Arabia

<sup>2</sup> Physics Department, Faculty of Science, Ain Shams University, Cairo, Egypt

<sup>3</sup> Intelligent Construction Automation Center, Kyungpook National University, 80, Daehak-ro, Buk-gu, Daegu 41566, Republic of Korea

between the functionalities of organic polymers and inorganic nano materials. For instant, the optical, thermal and electrical features of polyethylene oxide and polyacrylamide: lithium bromide polymer electrolyte films were improved as it loaded with nano silver [8]. The enhancements in optical characteristics, thermal stability, and A.C. conductivity of CMC as the amount of ZnO/Co increased strong support for the employ of the nanocomposite films in the solid state battery applications [3]. The optical features of polyvinyl pyrrolidone were modulated via praseodymium (III) nitrate salt doping [9]. The band gap of polyvinylcarbazole (PVK) polymer was rose as it loaded with nano ZnS doped with Mn, Fe, Cu or Ag while the quenching in the luminescence is increased as PVK loaded with ZnS:Mn [10]. The different dispersion parameters of  $Zn_{0.75-x}Cd_{0.25}V_xS/PVA/PVP$  were affected by the content of vanadium [11]. The optical band gap of PVA/PVP/PEG polymer blend decreased from 5.32 to 4.48 eV and 4.16 eV as the blend loaded with 10% CdS/Mg (air, 10 nm) and 5% CdS/Mg ( $N_2$ , 17 nm), respectively [12]. The nonlinear optical parameters were enhanced as PVA/PVP/PEG polymer loaded with CdS/Mg ( $N_2$  or air) [12]. The thermal stability of PVA was enhanced as it loaded with  $Zn_{0.99}Cu_{0.01}S$  [13]. The optical characteristics of PVA were affected by crystallite size of annealed ZnS nano filler [14]. The rates of decline in the direct and indirect optical band gaps of PVA/PVP blend doped with CdS/Fe (air, smaller crystallite size) are higher than the polymer blends doped with CdS/Fe ( $N_2$ , larger crystallite size) [15]. The nonlinear parameters for the PVA/PVP/CdS/Fe ( $N_2$ ) have nearly fixed values over a wide range of wavelengths as compared with blend doped with CdS/Fe (air) [15].

Therefore, annealing or preparation temperatures of the nano filler influence the properties of the host blends. Also, the optical band gap of the host polymer blend was affected by the crystallite size/amount of defects in the nanofiller. Furthermore, the kind of the doping element in the nanofiller affects its features and hence affects the characteristics of the host polymer.

The aim of the current study has been concerned with the investigation of structural, thermal, linear and nonlinear optical characterization of PVA/CMC blend loaded with different crystallite size from  $Zn_{0.9}V_{0.1}S$  nanoparticles using X-ray diffraction, Fourier transform infrared (FTIR) spectroscopy, thermogravimetric analysis, scanning electron microscope, diffused reflectance and luminescence spectrophotometer techniques.

## Materials and methods

$Zn_{0.9}V_{0.1}S \equiv ZnS/V$  samples were formed by mixing and grinding a stoichiometric ratios (1:1) from (zinc acetate and ammonium metavanadate): thiourea. The mixture was divided into several portions and each portion was heated at

200, 300, 400 or 500 °C (120 min) in an electric furnace, separately.

PVA/CMC (80/20%) and polymer blend was created using casting process; 0.8 g of polyvinyl alcohol (PVA) and 0.2 g of carboxymethyl cellulose (CMC) (in the form of the sodium salt of commercial grade) were dissolved in 80 and 20 ml distilled water under stirring at 70 and 50 °C, respectively, until a clear solutions were formed. The created solutions were mixed and stirred together at 50 °C (180 min). The resulted solution was placed in a Petri dish and located in an oven for 5 days at 45 °C. The above steps were repeated but in the present of 5 wt% from ZnS/V prepared at different temperatures. The formed blends have a thickness of 170–220  $\mu m$  (digital micrometer with accuracy  $\pm 1 \mu m$ ). The weight ratio between the nanofiller and the polymer blends (0.05:1) are calculated using the following relation:

$$x(\text{wt}\%) = \frac{w_f}{w_p + w_f} \times 100 \quad (1)$$

where  $w_f$  and  $w_p$  are the weights of nanofiller and polymer blend, respectively.

X-ray diffraction data were collected by a PANalytical diffractometer (X'pert MPD, Philips, copper source) device. The fluorescence and UV diffused spectra were conducted using a luminescence spectrophotometer (FP-8200 JASCO) and diffused reflectance spectrophotometer technique (JASCO-V-670) with attached integrating sphere assembly devices. Fourier transform infrared (FTIR) spectroscopy (Bruker Tensor 27 FTIR Spectrometer), scanning electron microscope (JEOL, Akishima, Tokyo, Japan JED-2200 Series) were used to inspect the morphology compositions and vibration bands of different blends. Thermogravimetric analysis (TGA) curves were got employing a Shimadzu TGA-50 thermogravimetric analyzer maintaining the heating temperature range between 25–800 °C at a rate of 20 °C  $\text{min}^{-1}$  using  $N_2$  environment.

## Results and discussion

### Structure and morphology investigations

The x-ray diffractions patterns recorded for the nanofiller  $Zn_{0.9}V_{0.1}S$ , Fig. 1a, resemble single phase ZnS of cubic zincblende structure, certifying that V ions diffused into the lattice substitutionally for Zn ions or interstitially at the lattice voids. The diffraction peaks are broad indicating that crystallite size of the prepared samples in the nano range [5]. The influence of preparation temperature on the cell parameter, the crystallite size, and the lattice microstrain is traced applying Rietveld refinement, Table 1. Figure 1b depicts the resulting diffraction pattern fitting for the sample

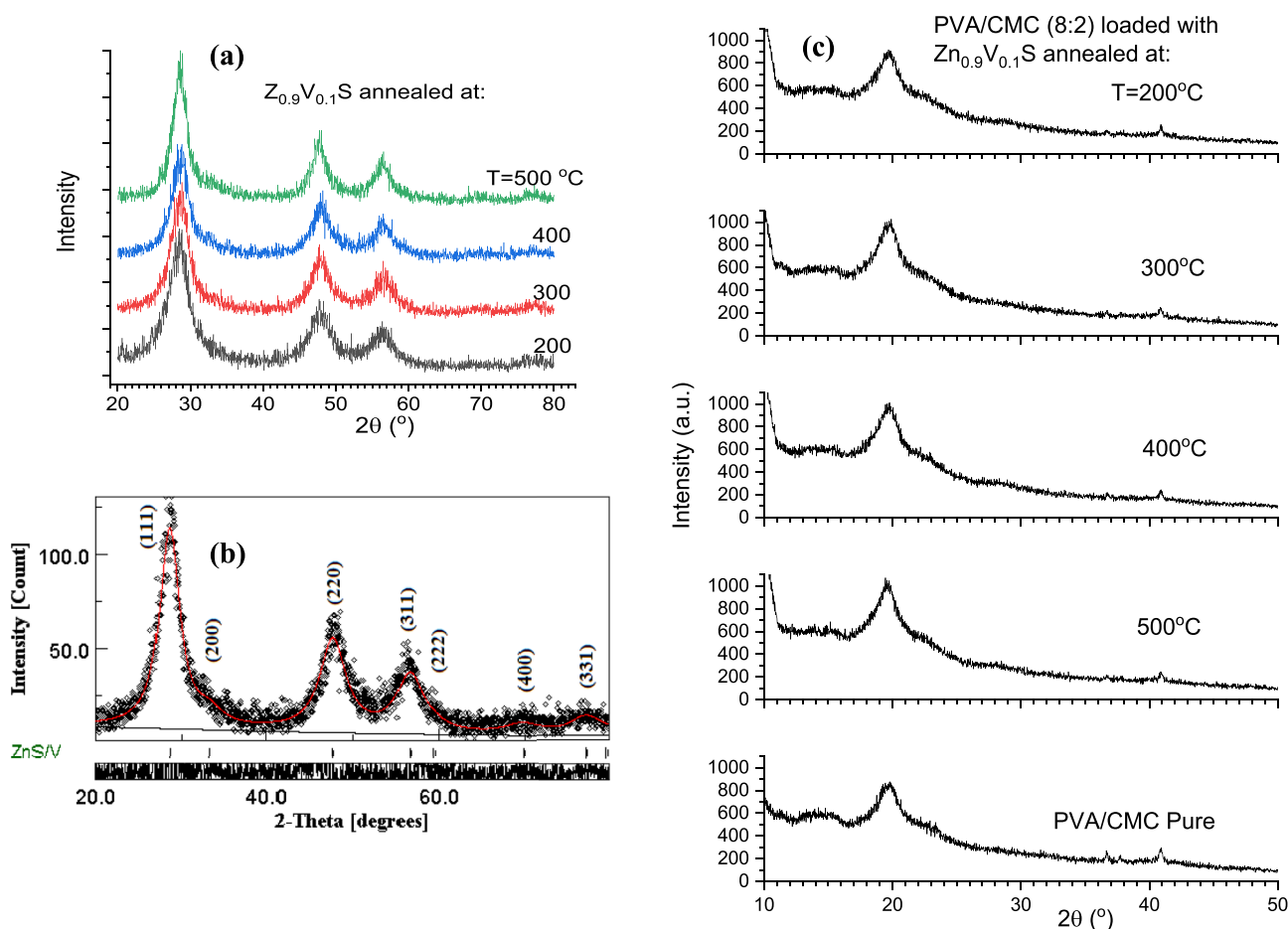


**Fig. 1** (a) XRD for ZnS/V prepared at different temperatures, (b) Rietveld refinement for ZnS/V prepared at 300 °C and (c) pure and doped PVA/CMC polymer blends with ZnS/V prepared at different temperatures

prepared at 300 °C. Analysis revealed crystallite size in the nano range for all samples and that the size increased with increasing the preparation temperature, Table 1. This is consistent with the fact that high preparation temperature would result in agglomeration of individual grains; by rising the preparation temperature, a sufficient thermal energy is supplied, which enables the coalescence of the adjacent crystallites and results in grain growth [16]. The r.m.s. lattice microstrain is reduced upon raising the temperature of preparation, indicating a reduction in lattice defects. This may be correlated with the decrease in cell parameter (*a*)

**Table 1** Lattice parameter (*a*), crystallite size and strain for annealed Zn<sub>0.9</sub>V<sub>0.1</sub>S nano samples

Temp °C	<i>a</i> Å	Size nm	Strain $\times 10^{-3}$
200	5.339(1)	3.1	12
300	5.359	3.7	8.8
400	5.366	3.6	6.2
500	5.385	4.7	3.3

is with temperature of preparation, Table 1. Typically, ZnS nanostructure retains several defects for instance sulfur vacancies, interstitials, stacking fault, etc., which produce lattice distortions and change the lattice parameters. Lattice vacancies tend to reduce the unit cell while interstitial defects increase the unit cell. These defects are reduced because of the increasing of the temperature of preparation, and the lattice contracts.

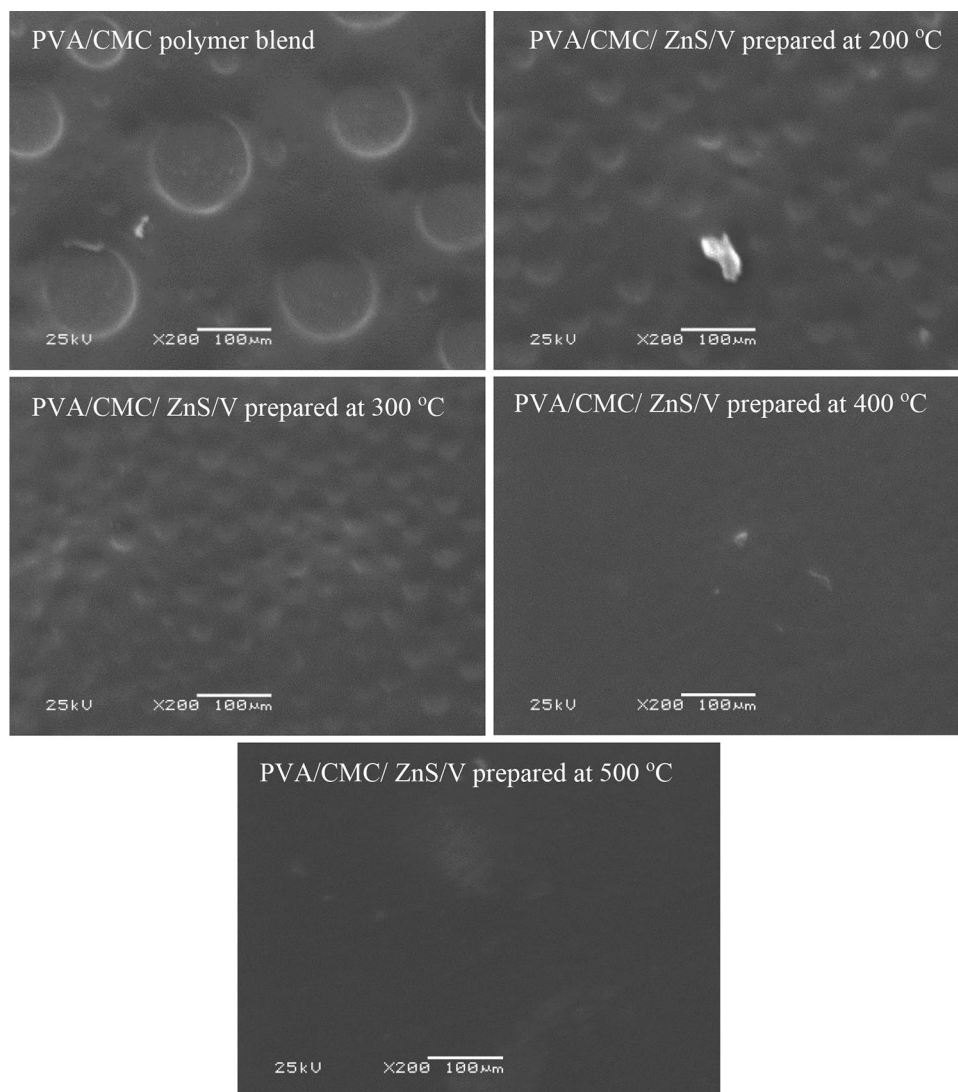
The x-ray diffractograms recorded for the polymer's blends PVA/CMC (8:2) pure and loaded with Zn<sub>0.9</sub>V<sub>0.1</sub>S annealed at different temperatures are depicted in Fig. 1c. The diffraction peaks characterizing Zn<sub>0.9</sub>V<sub>0.1</sub>S couldn't be detected in all diffraction patterns, indicating the well dispersion of the nanofiller through the polymers matrix and all patterns resemble the features of the polymer's blend. Moreover, since CMC is typically amorphous polymer that exhibits a hump at around 20° [17, 18], all peaks appeared at 19.5°, 20.1°, and 23.0° are the characteristic peaks (10  $\bar{1}$ ), (101) and (200) of the polymer PVA, respectively [19, 20]. The peak at around 40.5° corresponding to overlapping of (111), (1  $\bar{1}$  1), (210), and (2  $\bar{1}$  0) PVA planes [20].

The changes in the surface morphology of the polymer blend upon loading with  $Zn_{0.9}V_{0.1}S$  were tracked by SEM images. Pure polymer blend exhibited a surface with large pores resulted from the slow evaporation of the solvent [21], Fig. 2a. When the polymer blend cools and solidifies, gas bubbles form and appear as rounded, circular cavities or pores. The pores size reduced while their numbers increased upon loading the nanofiller, Fig. 2b-c. The particle size of  $Zn_{0.9}V_{0.1}S$  seemingly affects the formation of holes during the casting process. As the temperature of preparation of  $Zn_{0.9}V_{0.1}S$  increased, its particle size and the holes formed during solvent evaporation decreased. Smooth film surfaces without pores were obtained for the films loaded with  $Zn_{0.9}V_{0.1}S$  prepared at 400 or 500 oC. The energy dispersive X-ray analysis (EDS) spectra for pure and doped PVA/CMC blends ZnS/V (prepared at 400 °C as an example) are shown in Fig. 3. The source of sodium (Na) in the EDS spectra for both samples is

resulted from the used sodium carboxymethyl cellulose (CMC) polymer which is utilized in the manufacture of PVA/CMC blend. The corresponding EDS results point out the good matching with the elemental composition of the pure and doped polymer blends.

Figure 4 represents the FT-IR transmission data for pure and doped PVA/CMC polymer blends with ZnS/V prepared at different temperatures. As noticed from the graph, small modifications in the location and intensities of the vibrational band of the pure blend were detected as it loaded with ZnS/V prepared at different temperatures, Table 2. These modifications are due to the replacement of some carbon and nitrogen atoms with the nanofiller in the backbone of the formed polymer. As revealed from the graph, the OH stretching band is represented by the band at  $3827\text{ cm}^{-1}$  [22].  $C\equiv C$ ,  $C\equiv N$  and  $(C=O)$  and  $(COO^-)$  groups for PVA and CMC bonds are situated at  $2264$ ,  $2115$  and  $1986\text{ cm}^{-1}$ , respectively [23–25].

**Fig. 2** SEM images for pure and doped PVA/CMC polymer blends with ZnS/V prepared at different temperatures



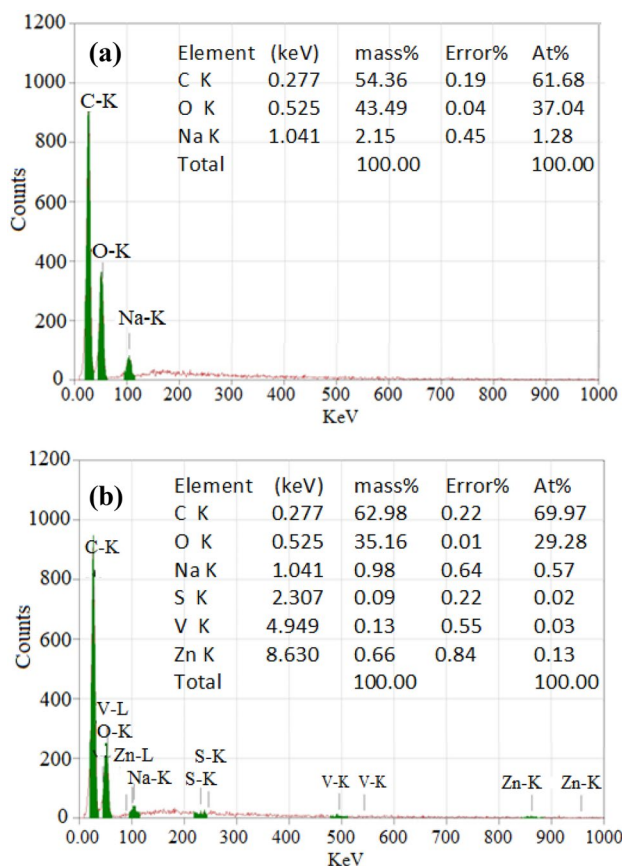


Fig. 3 EDS data for (a) pure and (b) doped PVA/CMC polymer blends with ZnS/V prepared at 400 °C

**Thermal properties**

Figure 5a, b displays the plots of the thermogravimetric analysis (TGA) and the 1<sup>st</sup> derivative of TGA (DTA) for pure and

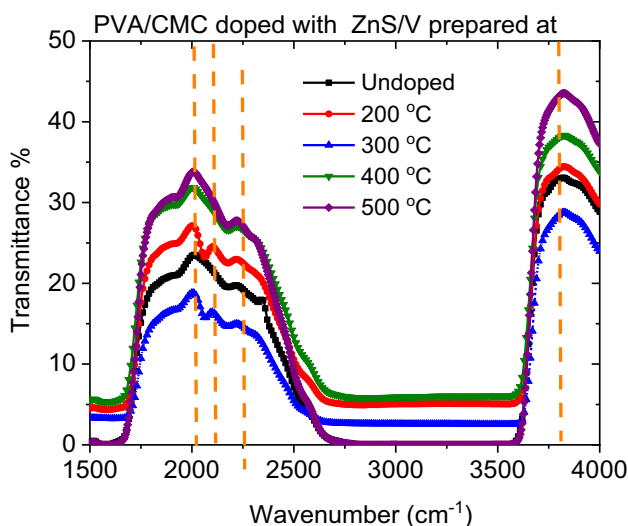


Fig. 4 FTIR for pure and doped PVA/CMC polymer blends with ZnS/V prepared at different temperatures

**Table 2** Locations of FTIR bands in pure and doped PVA/CMC polymer blends with ZnS/V prepared at different temperatures

PVA/CMC/ ZnS/V prepared at different temperature	IR bands (cm <sup>-1</sup> )			
	1878	2027	2210	3805
Pure				
200 °C	1861	1994	2226	3823
300 °C	1878	1994	2209	3823
400 °C	1845	1994	2226	3823
500 °C	1894	2011	2210	3823

doped PVA/CMC polymer blends with ZnS/V prepared at different temperatures. The TGA and 1<sup>st</sup> derivative of TGA figures revealed that the loss of mass in the range between 25 and 200 °C resulted from the evaporation of moisture/solvent and partial dehydration of blend chain [26, 27]. As demonstrated from Table 3, all samples exhibited different decompositions states (T<sub>d1</sub>, T<sub>d2</sub>) resulted from the arrangement of the polymer structure and the decomposition of the

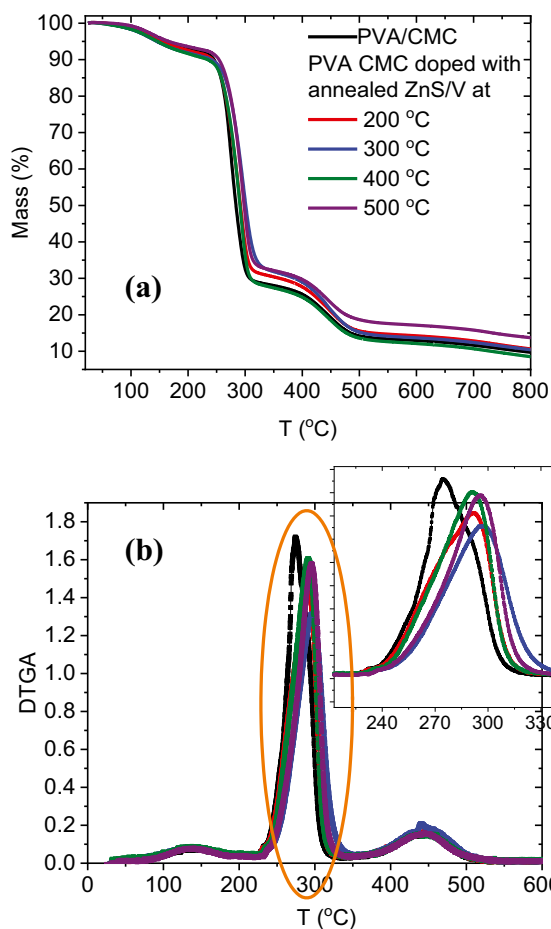


Fig. 5 (a) TGA and (b) DTG thermograms for pure and doped PVA/CMC polymer blends with ZnS/V prepared at different temperatures

**Table 3** TGA data for pure and doped PVA/CMC polymer blends with ZnS/V prepared at different temperatures

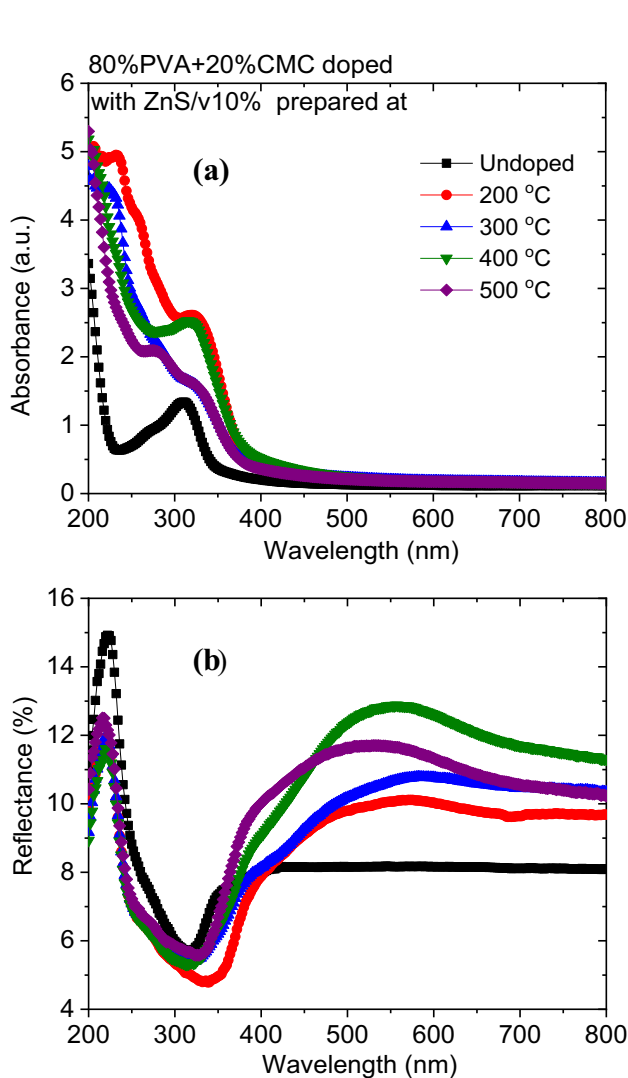
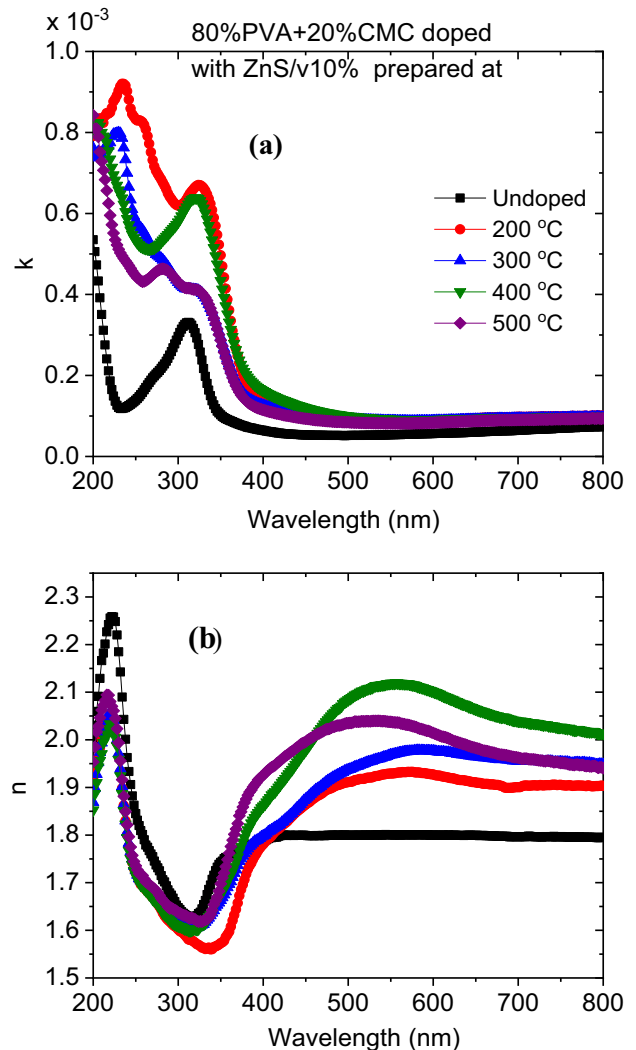
PVA/CMC/ ZnS/V prepared at different temperature	$T_{d1}$ (°C)	$T_{d2}$ (°C)	$T_{50}$ (°C)
Pure	275	451	284
200 °C	293	450	292
300 °C	298	449	301
400 °C	291	446	291
500 °C	294	444	298

blend, respectively [28–30]. The variation of the decomposition temperature is due to the insertion of ZnS/V into the PVA/CMC matrix which may affect the motions of polymer chains [30]. Furthermore the residual mass of doped blends

is higher than that the undoped blend owing to the interaction of ZnS/V with PVA/CMC chain made the blends prevented the condensation – degradation reaction [30]. In addition, the temperature at which 50% mass loss in different blends takes place is represented in Table 3. As demonstrated from the table, all doped blends have a higher thermal stability than the pure one and attained its highest stability as the blend loaded with ZnS/V prepared at 300 °C. The last stage between 500–800 °C, represented the decomposition of the blend and converted to carbonaceous matter [30].

### UV- Spectroscopy characteristics

The optical diffused absorption (A) and reflectance (R) spectra for pure and doped PVA/CMC polymer blends with ZnS/V prepared at different temperatures were collected

**Fig. 6** (a) Absorbance and (b) reflectance spectra for pure and doped PVA/CMC polymer blends with ZnS/V prepared at different temperatures**Fig. 7** Changing in the (a) extinction coefficient and (b) refractive index vs. incident wavelength for pure and doped PVA/CMC polymer blends with ZnS/V prepared at different temperatures

and depicted in Fig. 6. In the absorbance spectra there are three absorbance bands at 200–232, 280 and 313–323 nm which appeared depended on the present of nanofiller or not and also the crystallite size of the nanofiller. The first band defined as the  $n-\pi^*$  transition, which result from unsaturated C=O and/or C=C bonds that present in the tail-head of PVA [31]. The second and third bands associated to  $\pi-\pi^*$  transition, which is coming from the charge transfer group [32]. Furthermore, the intensities of these bands were raised as the blend doped with the nanofiller. All blends have no any absorption peak in the visible range, owing to their high transparency. The variations in the reflectance data upon loaded the PVA/CMC matrix with ZnS/V (prepared at different temperatures) may result from the alteration of the packing density of host PVA/CMC matrix [33].

The extinction coefficient ( $k$ , calculated using relation in Ref. [34]) and refractive index ( $n$ , calculated using relation in Ref [34].) for pure and doped PVA/CMC polymer blends with ZnS/V prepared at different temperatures were illustrated in Fig. 7. The graph indicated that the  $k$  value of PVA/CMC blend was increased as the blend loaded with ZnS/V and achieved the highest  $k$  value as it loaded with ZnS/V (prepared at 200 °C). In the UV range, the  $n$  value of pure blend is higher than the doped ones while in the visible range the situation is reversed. Blend with ZnS/V (prepared at 400 °C) has a highest  $n$  value. Similar results were observed as PVA loaded with different phases from  $\text{TiO}_2$  [35]. This variation of  $n$  values may result from the variation of density and polarization of the blend upon loaded with the nanofiller caused by the intermolecular

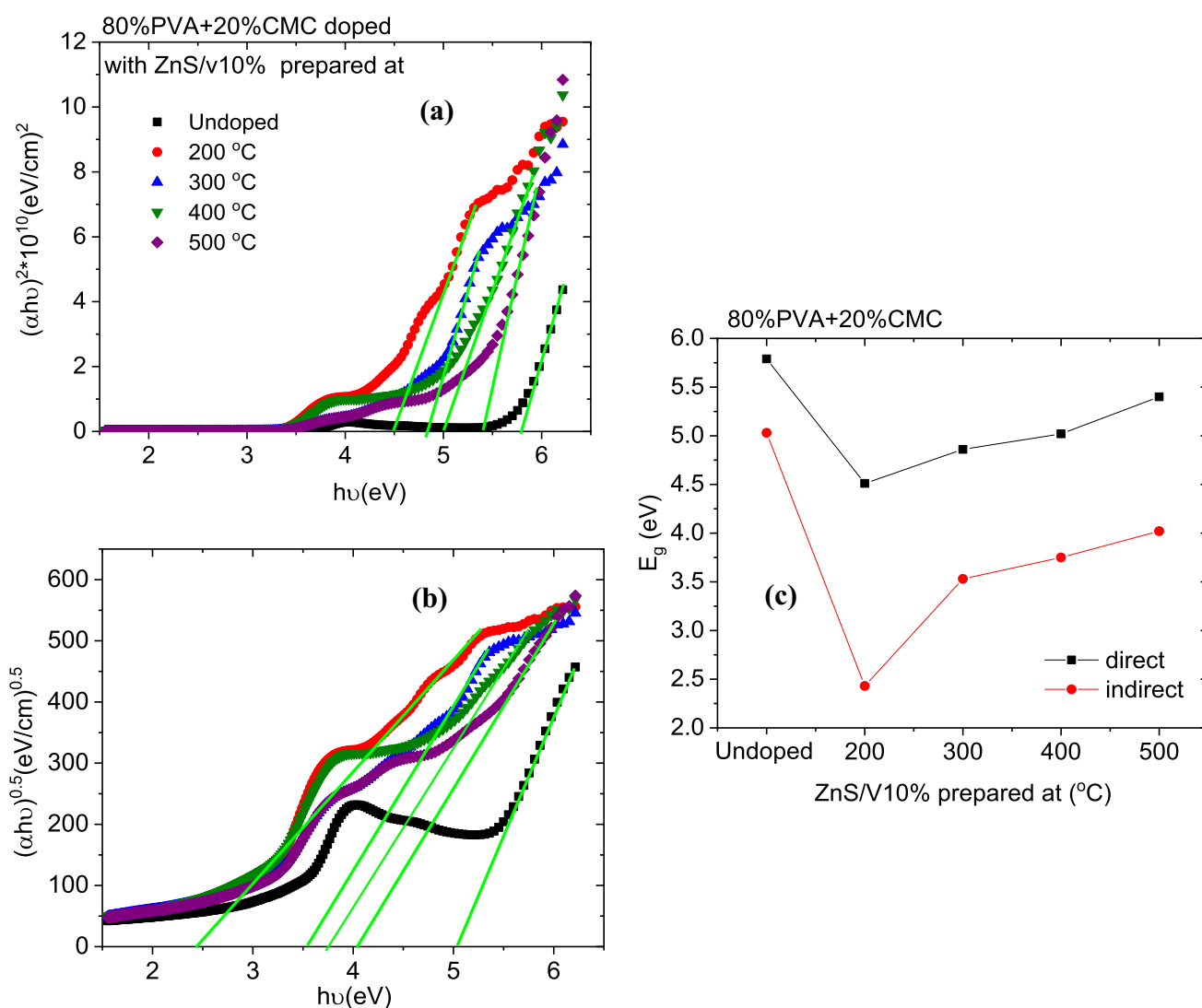


**Fig. 8** Plots of (a)  $(\alpha h\nu)^2$ , (b)  $(\alpha h\nu)^{0.5}$  vs.  $h\nu$  for pure and doped PVA/CMC polymer blends with ZnS/V prepared at different temperatures and (c) variation of the optical bandgap with ZnS/V prepared at different temperatures

interactions between the metallic fractals of embedded nanofillers and hydroxyl groups of the polymeric host [35, 36].

The optical energy gaps ( $E_g$ ) values can be found using the Tauc relation [37]:

$$ah\nu = B(h\nu - E_g)^m \quad (2)$$

$$\alpha (= A/d) \quad (3)$$

where  $h$ ,  $\nu$ ,  $B$ ,  $\alpha$  and  $d$  are Planck's constant, the frequency of the incident light, a constant, absorption coefficient and thickness of the film, respectively.  $m = 0.5$  or  $2$  for direct or indirect allowed transitions, respectively.

The allowed direct or indirect optical energies ( $E_g$ ) were calculated by extrapolating the linear part of the  $(ah\nu)^2$  or  $(ah\nu)^{0.5}$  versus the photon energy ( $h\nu$ ) curves to zero

absorption as displayed in Fig. 8a, b, respectively. The obtained direct and indirect optical band gaps are shown in Fig. 8c. As revealed from the graph, the direct and indirect  $E_g$  values for PVA/CMC are 5.79 and 5.03 eV. These energies were reduced as the blend doped with ZnS, Table 1. The lowest obtained optical band gap values (direct = 4.51 eV, indirect = 2.43 eV) as the blend doped with ZnS/V (prepared at 200 °C). Similar result was detected as PVA loaded with carbon quantum dots [31]. As the preparation temperature of the nanofiller increased, the direct and indirect optical band gaps increased. The reduction in  $E_g$  value upon loading the blend with ZnS/V nano filler indicated the increase the degree of disorderness which caused a creation of localized states between HOMO (highest-occupied molecular orbital) and LUMO (lowest unoccupied molecular orbital) bands of the host blend and also the modulation of the blend

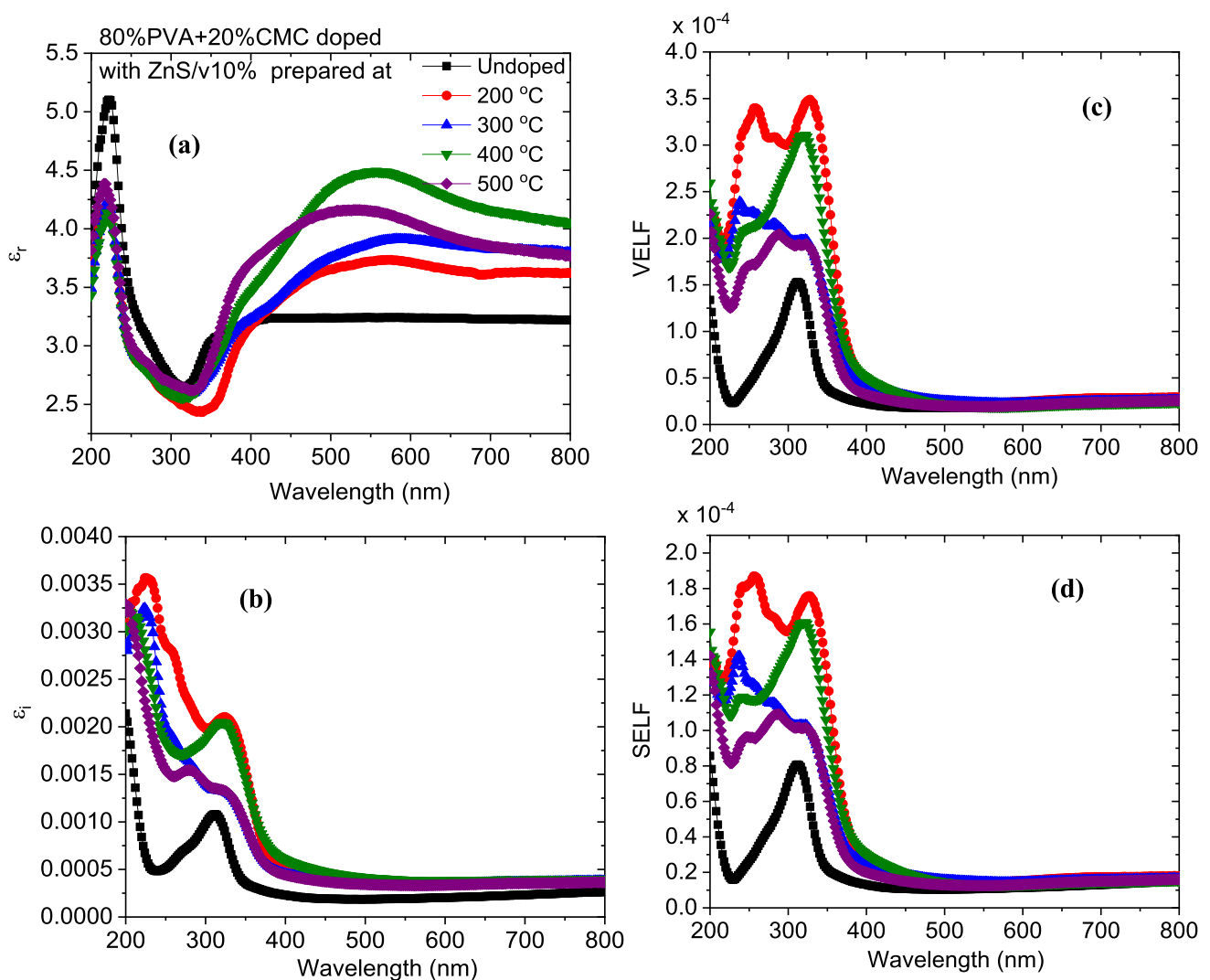


**Fig. 9** Wavelength dependent of the (a) real and (b) imaginary dielectric constant, (c) SELF and (d) VELF for pure and doped PVA/CMC polymer blends with ZnS/V prepared at different temperatures



structure upon insertion of the nanofiller [38]. Similar result was noticed as PVA loaded with sodium doped dysprosium oxide ( $\text{Na}_2\text{Dy}_2\text{O}_4$ ) nanofillers [36]. This reduction in  $E_g$  value demonstrated the ability of the loaded blends with the nanofiller to absorb more energy from the solar radiation from other wavelength ranges.

The real and imaginary parts ( $\epsilon_r$  and  $\epsilon_i$ , calculated using relations in Ref [34].) of optical dielectric constants have a relation with the energy densities of states within the optical energy gap of samples [34]. The variations of  $\epsilon_r$  and  $\epsilon_i$  and also the surface energy loss function (SELF, calculated using relation in Ref [34].) and volume energy loss function (VELF, calculated using relation in Ref [34].) with the wavelength for all blends are shown in Fig. 9. The enhancement in  $\epsilon_r$  of the doped blend as compared with pure blend in UV range indicated the reduction in the propagating of the light velocity through the blend. In the whole range,  $\epsilon_i$  values of the doped blends are higher than the pure blend due to the polymeric dipoles [36]. In the visible range,  $\epsilon_r$  increased irregularly and attained its highest value as the blend loaded with ZnS/V prepared at 400 °C. In UV range,  $\epsilon_i$  reduced regularly while in the visible range the variation is slightly as ZnS/V preparation temperature increased. Additionally, both SELF and VELF spectra displayed a similar trend. The values of VELF are higher than the values of SELF in the same blend. Doped blends have SELF and VELF in doped blends higher than the undoped blend. Blend with ZnS/V prepared at 200 °C has highest SELF and VELF values.

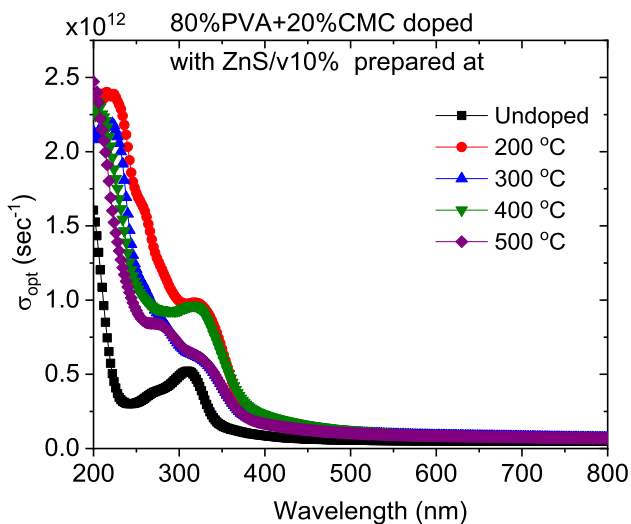


**Fig. 10** Optical conductivity plot for pure and doped PVA/CMC polymer blends with ZnS/V prepared at different temperatures

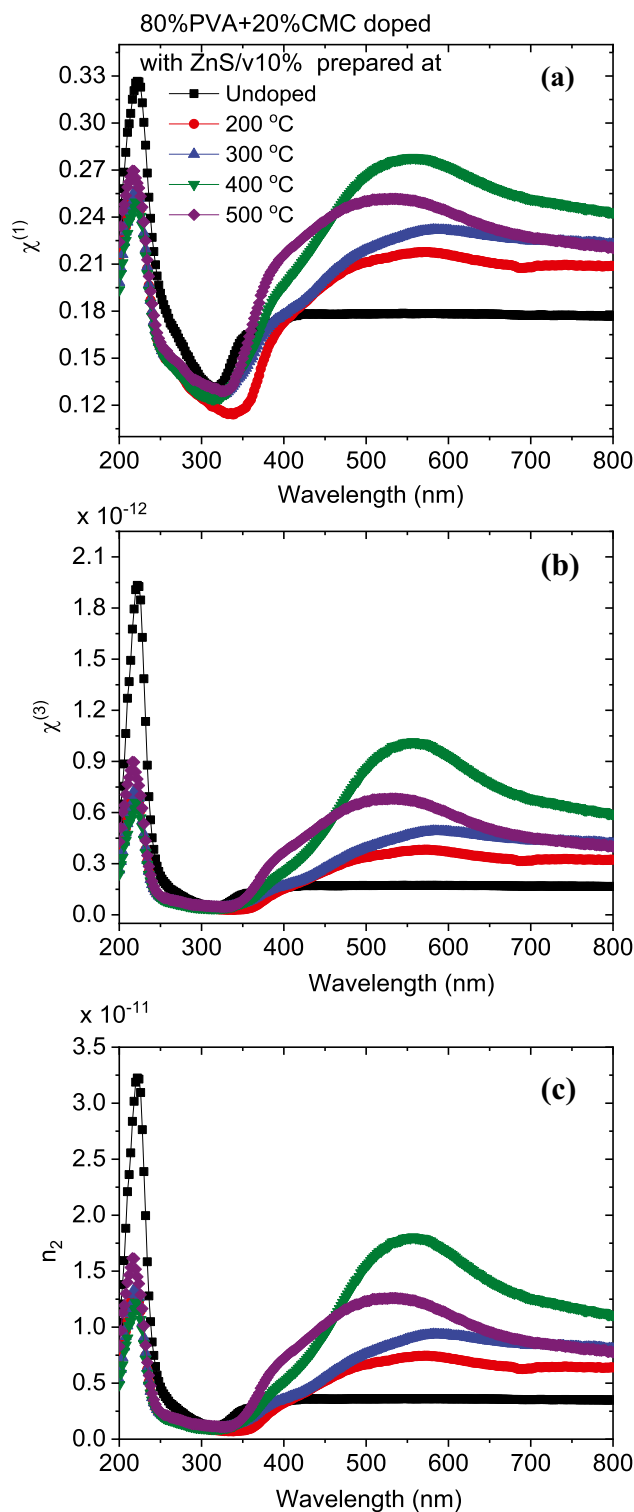


**Fig. 11** Variation of the (a) linear optical susceptibility, (b) nonlinear third order and (c) nonlinear refractive index for pure and doped PVA/CMC polymer blends with ZnS/V prepared at different temperatures

Optical conductivity ( $\sigma_{opt}$ , calculated using relation in Ref. [34]) represented the conduction performance of the materials as a result of the movement of charge carriers caused by applied electric field of the incident electromagnetic wave. The changes of  $\sigma_{opt}$  with the wavelength for all blends are revealed in Fig. 10. As noticed from the graph the optical conducting behavior of pure blend was increased as it loaded with the ZnS/V due to the raise in the charge carrier amount with ZnS/V nano inclusions. Similar result was observed as PVA loaded with different phases from  $\text{TiO}_2$  or  $\text{Na}_2\text{Dy}_2\text{O}_4$  [35, 36]. Additionally, the integrated nano filler caused creation of charge transfer complexes facilitating a novel conduction channel for the crossover of electrons between the various electronic states (HOMO/LUMO) states causes a reduction in the optical band gaps and hence improved the optical conductivities [39]. Therefore, these variations in the electric properties of the blend

upon loaded with the nanofillers nominated them to utilize in several optoelectronic applications.

Figure 11 displays the first and third orders optical susceptibility ( $\chi^{(1)}$ ,  $\chi^{(3)}$ ) and nonlinear refractive index ( $n_2$ ) (calculated from relations in Ref. [34]) for undoped and doped blends. As demonstrated from the plot, in the UV regions, the nonlinear optical parameters (NLO) values of the pure blend were reduced as it loaded with ZnS/V filler. In the visible range, the situation is reversed and the NLO of the doped blends enhanced as compared with undoped blend. Blend with ZnS/V prepared at 400 °C has a highest NLO values while blend doped with ZnS/V prepared at 200 °C has a lowest ones. The development of the NLO features of doped blends upon laded with ZnS/V nominates the formed blends to utilize in many communication and switching applications.

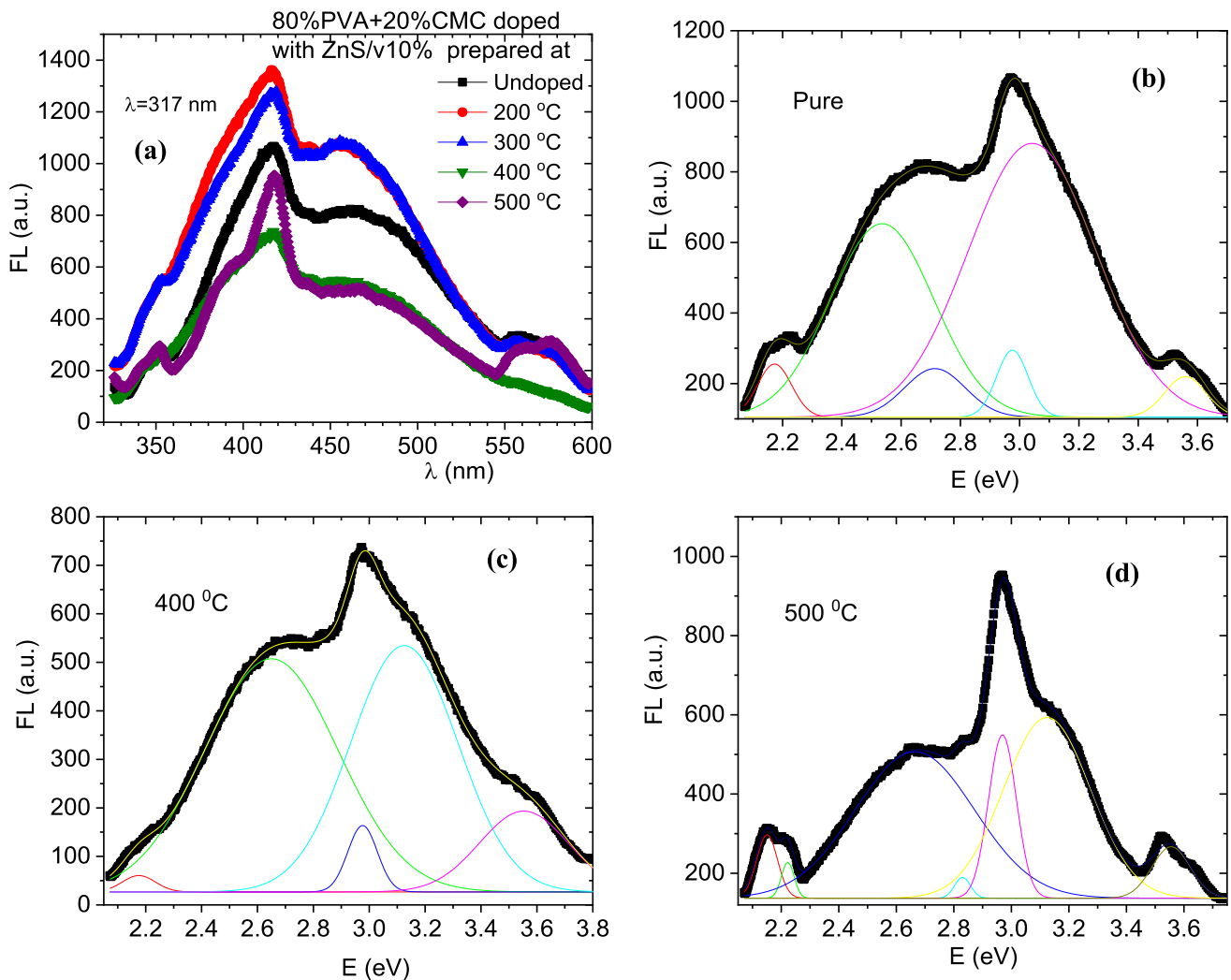


**Fig. 12** (a) The FL spectra for pure and doped PVA/CMC polymer blends with ZnS/V prepared at different temperatures and (b) the Gaussian fitting for pure and doped PVA/CMC polymer blends with ZnS/V prepared at different temperatures

## Fluorescence (FL) properties

Figure 12a represents the FL spectra for pure and doped 80%PVA/20%CMC polymer blends with ZnS/V prepared at different temperatures under 317 nm. As shown from the graph the full width at half maximum intensity (FWHM) of the FL spectra of the pure blend became broader as it doped with ZnS/V prepared at 200 °C. The broadening of the spectra indicated more defect centers were created within the blends upon doped with the nanofiller. Furthermore, as the preparation temperature of ZnS/V increased the FWHM of the doped blends became less broad which demonstrated the reduction of the number of defects inside the blend. As demonstrated from XRD analysis the nano size of ZnS/V was increased as the preparation temperature increased and hence the defects reduced. In addition the intensity of FL spectra was improved as the pure blend doped with ZnS/V prepared at 200 °C, then reduced with further increasing in the preparation temperature of the nanofiller. The enhancement or deenhancement in the FL intensity as the blend doped with ZnS/V prepared at different temperature may result from raising or reduction in the recombination rate of the photo-induced electrons and holes pairs inside the different blends [40, 41]. The decreasing and increasing in the FL intensity, nominated the loaded blends to be employed in photocatalytic degradation of organic dyes and optoelectronic application, respectively. In order to explore the effect of ZnS/V doping on the emitted colors of the pure blend (UV, two violets, two blues, green), Gaussian fitting was employed. The doped blend with ZnS/V prepared at (200, 300, 400, 500) °C showed (UV, two violets, two blues, green), (UV, two violets, two blues, green), (UV, two violets, blue, green) and (UV, two violets, two blues, green, yellow) colors, respectively. The UV and violet colors were formed from the transfer of the electrons from near band emission (NBE) and the excitonic transitions [40]. The blue emission is caused by the defect-related luminescence and dopant/impurity atoms, respectively [40]. The yellow color may be created from the electronic movement from  $Zn_i$  to (ionized oxygen vacancies)  $O_i$  states [42]. The loaded blends can be applied in ptoelectronic, communication, switching applications and photocatalytic degradation of organic dyes.

## Conclusion

All nanofillers samples  $Zn_{0.9}V_{0.1}S$  have single phase ZnS of cubic zincblende structure in the nano range. The lattice microstrain and lattice parameter of ZnS/V are reduced upon raising the temperature of preparation. The pure polymer blend PVA/CMC exhibited a surface with large pores. The pores size reduced while their numbers increased upon loading the nanofiller. Smooth film surfaces without pores were

obtained for the films loaded with ZnS/V prepared at 400 or 500 °C. All doped blends have a higher thermal stability than the pure one and attained its highest stability as the blend loaded with ZnS/V prepared at 300 °C. The refractive index ( $n$ ) varied nonlinearly with wavelength, attaining values for the pure blend larger than for doped ones in the UV range, but smaller in the visible range. The direct and indirect  $E_g$  values of the doped blends decreased nonmonotonically with nanofiller preparation temperature, attained their lowest values for  $T=200$  °C. Upon loading,  $\epsilon_r$  and NLO parameters increased, in the visible range, irregularly with nanofiller preparation temperature, attaining highest values for  $T=400$  °C. The optical conductivity increased also irregularly. The FL intensity was improved as the pure blend doped with ZnS/V prepared at 200 °C, then reduced with further increasing in the preparation temperature of the nanofiller. Pure blend emitted (UV, violet, blue, green) colors while doped blends exhibited (UV, violet, blue, green, yellow) colors depended on the preparation temperature of the ZnS/V.

**Acknowledgements** This work is supported by Researchers Supporting Project number (RSP-2021/72), King Saud University, Riyadh, Saudi Arabia.

## References

- Chai L, Zhong M, Li X, Wu N, Zhou J (2018) Superlattices Microstruct 120:279
- Singh R, Kulkarni SG, Channe SS (2013) Polym Bull 70:1251
- Abutalib MM, Rajeh A (2020) Polym Test 91:106803
- Zahan M, Islam MR, Podder J (2019) Indian J Phys 93:611
- Heiba ZK, Mohamed MB, Badawi A (2022) Appl Phys A 128:456
- Rana MS, Das SK, Md O, Rahman FA, Md A, Hossain, (2021) Trans Electr Electron Mater 22:612
- Heiba ZK, Mohamed MB, Badawi A (2022) Appl Phys A 128(5):1
- Morsi MA, El-Khodary SA, Rajeh A (2018) Phys B: Condens Matter 539:88
- Mahmoud KH, Alsubaie ASA, Elsayed KA (2021) Optik 231:166383
- Sharma K, Kumar P, Verma G, Kumar A (2020) Optik 206:164357
- Heiba ZK, El-naggar AM, Mohamed MB, Kamal AM, Osman MM, Albassam AA, Lakshminarayana G (2022) Opt Quant Electron 54:452
- El-naggar AM, Heiba ZK, Mohamed MB, Kamal AM (2022) J Mater Sci: Mater Electron 33:17235
- Mohamed MB, Heiba ZK, Imam NG (2018) J Mol Struct 1163:442
- Mohamed MB, Abdel-Kader MH (2020) Mater Chem Phys 241:122285
- Heiba ZK, El-naggar AM, Mohamed MB, Kamal AM, Osman MM, Albassam AA, Lakshminarayana G (2021) Opt Mater Part B 122:111788
- Koaib J, Bouguila N, Abassi H, Moutia N, Kraini M, Timoumi A, V´azquez-V´azquez C, Khirouni K, Alaya S (2020) RSC Adv. 10:9549
- Upadhyaya L, Singh J, Agarwal V, Pandey AC, Verma SP, Das P, Tewari RP (2014) J Polym Res 21:1

18. Megha R, Ravikiran YT, Kotresh S, Kumari SCV, Raj Prakash HG, Thomas S (2018) *Cellulose* 25:1147
19. Assender HE, Windle AH (1998) *Polymer* 39:4295
20. Ricciardi R, Auriemma F, De Rosa C, Laupretre F (2004) *Macromolecules* 37(5):5–1921
21. Baki Hazer J (2014) *Polym Environ* 22:200
22. Rajeswari N, Selvasekarapandian S, Sanjeeviraja C, Kawamura J, Asath Bahadur S (2014) *Polym Bull* 71:1061
23. Farah AM, Thema FT, Dikio ED (2012) *Int J Electrochem Sci* 7:5069
24. Xia Q, Zhao XJ, Chen SJ, Ma WZ, Zhang J, Wang XL (2010) *EXPRESS Polym Lett* 4(5):284
25. Morsi MA, Oraby AH, Elshahawy AG, Abd El-Hady RM (2019) *J Mater Res Technol* 8(6):5996
26. Premalatha M, Vijaya N, Selvasekarapandian S, Selvalakshmi S (2016) *Ionics* 22:1299
27. Budrugaec P (2008) *J Therm Anal Calorim* 92:291
28. Singh VK, Shalu SKC, Singh RK (2016) *RSC Adv* 6:40199
29. Singh P, Bharati DC, Gupta PN, Saroj AL, Non-Cryst J (2018) *Solids* 494:21
30. Mizanur M, Khan R, Pal S, Hoque MM, Alam MR, Younus M, Kobayashi H (2019) *ACS Omega* 4:6144
31. El-Shamy AG, Zayied HSS (2020) *Synth Met* 259:116218
32. El-Shamy AG, Maati AA, Attia W, Abd El-Kader KM (2018) *J Alloys Compd* 744:701
33. Kafashan H, Azizieh M, Vatan HN (2016) *J Alloy Comp* 686:962
34. El-naggar AM, Heiba ZK, Mohamed MB, Kamal AM, Lakshminarayana G (2022) *M AShar. Optik* 258:168941
35. Morad I, Alshehri AM, Mansour AF, Wasfy MH, El-Desoky MM (2020) *Physica B* 597:412415
36. Shilpa KN, Nithin KS, Sachhidananda S, Madhukar BS (2017) *Siddaramaiah. J Alloys Compd* 694:884
37. Tauc J, in: Abeles A (Ed.) (1972) *Op Proper Solid* p. 277. North Holland, Amsterdam
38. El-Shamy AG (2019) *J Alloys Compd* 810:151940
39. Forouhi AR, Bloomer I (1986) *Phys Rev B Condens Matter Mater Phys* 34:7018
40. Tao S, Zhu S, Feng T, Xia C, Song Y, Yang B (2017) *Mater Today Chem* 6:13
41. Raja G, Gopinath S, Azhagu R, Shukla AK, Alhoshan MS, Sivakumar K (2016) *J Phys E* 158:69
42. Wang HQ, Wang GZ, Jia LC, Tang CJ, Li GH (2007) *J Phys D Appl Phys* 40:6549

**Publisher's Note** Springer Nature remains neutral with regard to jurisdictional claims in published maps and institutional affiliations.

Springer Nature or its licensor (e.g. a society or other partner) holds exclusive rights to this article under a publishing agreement with the author(s) or other rightsholder(s); author self-archiving of the accepted manuscript version of this article is solely governed by the terms of such publishing agreement and applicable law.